

## Topological Superconductivity and Majorana Fermions in RKKY Systems

Jelena Klinovaja,<sup>1,2</sup> Peter Stano,<sup>1,3</sup> Ali Yazdani,<sup>4</sup> and Daniel Loss<sup>1</sup>

<sup>1</sup>*Department of Physics, University of Basel, Klingelbergstrasse 82, CH-4056 Basel, Switzerland*

<sup>2</sup>*Department of Physics, Harvard University, Cambridge, Massachusetts 02138, USA*

<sup>3</sup>*Institute of Physics, Slovak Academy of Sciences, 845 11 Bratislava, Slovakia*

<sup>4</sup>*Joseph Henry Laboratories and Department of Physics, Princeton University, Princeton, New Jersey 08544, USA*

(Received 4 July 2013; published 1 November 2013)

We consider quasi-one-dimensional Ruderman-Kittel-Kasuya-Yosida (RKKY) systems in proximity to an  $s$ -wave superconductor. We show that a  $2k_F$  peak in the spin susceptibility of the superconductor in the one-dimensional limit supports helical order of localized magnetic moments via RKKY interaction, where  $k_F$  is the Fermi wave vector. The magnetic helix is equivalent to a uniform magnetic field and very strong spin-orbit interaction (SOI) with an effective SOI length  $1/2k_F$ . We find the conditions to establish such a magnetic state in atomic chains and semiconducting nanowires with magnetic atoms or nuclear spins. Generically, these systems are in a topological phase with Majorana fermions. The inherent self-tuning of the helix to  $2k_F$  eliminates the need to tune the chemical potential.

DOI: [10.1103/PhysRevLett.111.186805](https://doi.org/10.1103/PhysRevLett.111.186805)

PACS numbers: 71.10.Pm, 74.20.-z, 75.70.Tj, 75.75.-c

**Introduction.**—Majorana fermions (MFs) [1] have attracted wide attention due to their exotic non-Abelian statistics and their promise for topological quantum computing [2,3], also fueled by recent experiments searching for MFs [4–10]. The crucial ingredient for most MF proposals is helical spin textures leading to an exotic  $p$ -wave pairing due to a proximity effect with an ordinary  $s$ -wave superconductor [3,11–14]. The associated helical modes, which transport opposite spins in opposite directions, are proposed to exist in various systems [13–21]. A well-known mechanism responsible for helical modes is spin-orbit interaction (SOI) of Rashba type [3,11,12]. However, quite often, an external uniform magnetic field is needed, and the spin polarization of the helical modes is not ideal but depends on the SOI strength [15]. While intrinsic values of SOI are limited by material parameters, the recently proposed synthetic SOI produced by a helical magnetic field can reach extraordinary values that are limited only by the spatial period of the helical field  $2\pi/k_n$  [22]. Such helical fields can be engineered with nanomagnets [20–25] or, more atomistically, can emerge from helical spin chains due to anisotropic exchange and Dzyaloshinskii-Moriya interaction [26–29]. The equivalence between spectra of wires with intrinsic and with synthetic SOI has opened up new platforms for helical modes and MFs [20–24]. However, in all these setups, the chemical potential must be tuned inside the gap opened by the magnetic field so that the Fermi wave vector  $k_F$  is close to  $k_n/2$ . This poses additional challenges on experimental realizations by requiring wires with a high tunability of the Fermi level and high mobility down to ultralow densities.

Thus, it is natural to ask if helical modes exist in low-dimensional superconductors such that the system automatically tunes itself to  $k_n = 2k_F$ . Surprisingly, the answer turns out to be affirmative for a rather broad class of systems. These are RKKY systems that consist of localized

magnetic moments coupled by itinerant electrons via the Ruderman-Kittel-Kasuya-Yosida (RKKY) interaction [30–32]. It was recently discovered that in such systems, in the quasi-one-dimensional limit, the moments form a spin helix, leading to a Peierls-like gap at the intrinsic Fermi level such that  $2k_F = k_n$  [22,33–35]. However, these results were obtained for semiconducting or metallic systems in the normal phase, relying on the presence of gapless itinerant electrons to transmit the RKKY interaction. Thus, it is not clear that the same ordering mechanism can also develop in the superconducting regime where the spectrum of the electrons is gapped. In the present Letter, we address this issue in detail and demonstrate that the helical order arising from RKKY interaction also survives in one-dimensional (1D) superconductors. As a prototype for our model, we consider atomic chains [26] and semiconducting nanowires with magnetic atoms or nuclear spins placed on top of a bulk  $s$ -wave superconductor. We show that these setups are generically deep inside the topological phase and host MFs without requiring any fine-tuning at all.

**Model.**—We consider a quasi-1D superconducting wire aligned along the  $x$  axis with embedded localized magnetic moments; see Fig. 1. The quasi-one-dimensionality means

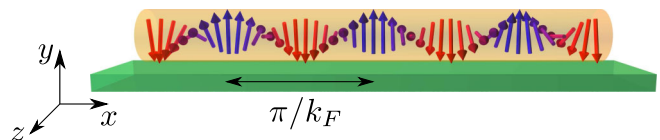


FIG. 1 (color online). Sketch of a one-dimensional system (yellow cylinder) aligned along the  $x$  axis brought into contact with an  $s$ -wave superconductor (green slab). Localized magnetic moments (arrows inside the cylinder) are ordered into a spin helix by RKKY interaction transmitted by electrons.

that only the lowest subband of the wire is occupied [36], and the wave function in the transverse direction is given by  $\psi(y, z) \equiv \psi(\mathbf{r}_\perp)$ . (A single subband is not crucial for what follows [35].) The 1D  $s$ -wave superconductor is described by the Hamiltonian

$$H = \int dx [\psi^\dagger \mathcal{H}_0(x) \psi + \Delta_s (\psi_\uparrow \psi_\downarrow + \text{H.c.})], \quad (1)$$

where  $\psi(x) = (\psi_\uparrow(x), \psi_\downarrow(x))$  with  $\psi_\sigma(x)$  being an annihilation operator acting on an electron at position  $x$  with spin  $\sigma$ . The superconducting coupling parameter  $\Delta_s \geq 0$  arises from the proximity effect. Here,  $\mathcal{H}_0(x) = -\hbar^2 \partial_x^2 / 2m - \mu_F$ , where  $m$  is the effective mass and  $\hbar \hat{k} = -i\hbar \partial_x$  the momentum operator. The energy is taken from the Fermi level  $\epsilon_k = \hbar^2(k^2 - k_F^2) / 2m$ , where the Fermi wave vector  $k_F = \sqrt{2m\mu_F} / \hbar$  is set by the chemical potential  $\mu_F$ . The quasiparticle energy in the superconductor is given by  $\eta_k = \sqrt{\epsilon_k^2 + \Delta_s^2}$ .

The interaction between itinerant electron spins and localized magnetic moments  $\tilde{\mathbf{I}}_i$  at position  $\mathbf{R}_i = (x_i, \mathbf{r}_{\perp,i})$  is described by the Hamiltonian density

$$\mathcal{H}_{\text{int}}(x) = \frac{\beta}{2} \sum_i \tilde{\mathbf{I}}_i \cdot \boldsymbol{\sigma} |\psi(\mathbf{r}_{\perp,i})|^2 \delta(x - x_i), \quad (2)$$

with the coupling strength  $\beta$  being a material constant. Here,  $\boldsymbol{\sigma}$  is the vector of Pauli matrices acting in electron spin space. In the following, we solve the interacting Hamiltonian  $H + H_{\text{int}}$  on a mean field level: We first integrate out the superconducting condensate in leading order  $\beta$  to derive an effective RKKY interaction for the subsystem of localized moments. We find its ground state and quantify conditions under which it is stable. Assuming these conditions are fulfilled, we derive an effective Hamiltonian for the electron subsystem.

**RKKY in a 1D superconductor.**—The localized moments spin-polarize the conducting medium, which influences other moments and results in the RKKY interaction. We now introduce an effective 1D model of magnetic moments, with a notation suitable for magnetically doped semiconductor wires, and extend it later to other realizations. We approximate the transverse wave function profile  $|\psi(\mathbf{r}_\perp)|^2$  by a constant, the inverse of the cross section area  $A$ . We assume there are  $N_\perp$  localized moments on a transverse plane. Although  $N_\perp$  might be large, once the magnetic order is established, these spins are collinear, since the spin excitations within the locked transverse plane are energetically much more costly than excitations we will consider below and can therefore be neglected [33]. Thus, a transverse plane is assigned a single (effective) spin of length  $I = N_\perp \tilde{I}$ . Neighboring planes are separated by a distance of the order of the lattice constant  $a$ , and the density of moments is parametrized as  $N_\perp = \alpha \rho_0 A a$ , with  $\alpha$  being the fraction of cations replaced by magnetic

atoms and  $\rho_0 = 4/a^3$  the cation density in zinc-blende materials.

With these definitions, the RKKY interaction between localized moments becomes

$$H^{\text{RKKY}} = - \sum_{i,j} J_{ij} \mathbf{I}_i \cdot \mathbf{I}_j, \quad (3)$$

where the long range coupling  $J_{ij} = -(2\beta^2/A^2)\chi(x_i - x_j)$  is given by the static spin susceptibility  $\chi$  of the 1D superconductor. In Fourier space,  $\chi_q = (1/a) \times \int dx \exp(iqx) \chi(x)$ , the susceptibility at zero temperature is given by [38]

$$\chi_q = - \frac{1}{4aL} \sum_k \frac{\eta_k \eta_{k+q} - \epsilon_k \epsilon_{k+q} - \Delta_s^2}{\eta_k \eta_{k+q}} \frac{1}{\eta_k + \eta_{k+q}}. \quad (4)$$

Here,  $L = Na$  is the system length. The finite temperature corrections to  $\chi$ , being exponentially small if  $\Delta_s \gg k_B T$ , are neglected. For a plot of  $\chi_q$ , see Fig. 2.

Although  $\chi_{q=0} = 0$  and thus the total magnetization is strictly zero [39], the superconductor responds at nonzero momenta  $q$ . If  $\Delta_s \leq \mu_F$ , the susceptibility develops a peak at  $q = 2k_F$ , which gets more pronounced as the ratio  $\Delta_s/\mu_F$  drops. Examining the limiting cases analytically, we suggest the following interpolation formula:

$$\chi_q \approx - \frac{k_F}{8\pi a \mu_F} \ln \left( \frac{e^{1/2+\gamma}}{\sqrt{\Delta_s^2/\mu_F^2 + (1 - q/2k_F)^2/2}} \right), \quad (5)$$

in the regime of  $\Delta_s \lesssim \mu_F$  and  $|q - 2k_F| \ll k_F$ . Here,  $\gamma \approx 0.58$  is the Euler gamma constant. Comparing to numerics, we find that it is an excellent approximation for the peak height at  $q = 2k_F$ , while away from this point it differs from the exact result by a broad nonresonant background only (see the insets of Fig. 2).

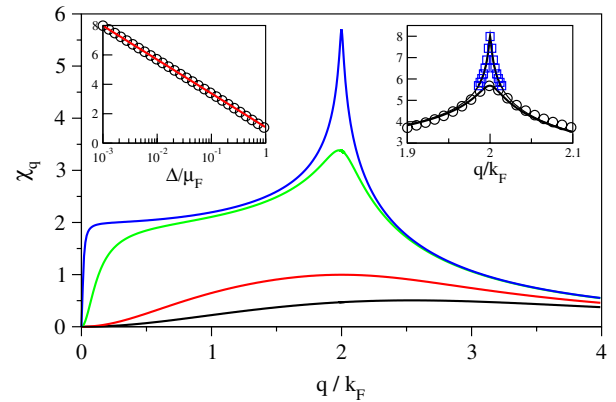


FIG. 2 (color online). One-dimensional superconductor susceptibility divided by  $k_F/8\pi a \mu_F$ . Main: Susceptibility given in Eq. (4) for  $\Delta_s/\mu_F = 2, 1, 0.1$ , and  $0.01$ , respectively (curves from the bottom up). Insets: Comparison of exact [symbols; Eq. (4)] and interpolation [solid line; Eq. (5)] values. Left: at  $q = 2k_F$ . Right: for  $\Delta_s/\mu_F = 0.01$  (circles) and  $0.001$  (squares).

The susceptibility peak, coming from the Fermi edge singularity, is known from normal systems. *A priori*, it is not obvious that a gapped system remains effective in mediating the RKKY exchange due to the cutoff introduced by the coherence length. Here, this is so, since the coupling range that is relevant is given by the Fermi wavelength, assumed to be much smaller than the coherence length,  $\Delta_s/\mu_F \ll 1$ .

*Magnons.*—The classical ground state of Eq. (3) with  $J$  peaked at finite momentum is a helically ordered pattern  $\mathbf{I}_i = \mathcal{R}_{\mathbf{h}, 2k_F x_i}[\mathbf{I}]$ , with  $\mathcal{R}$  a  $3 \times 3$  matrix corresponding to a vector rotation around the helical axis  $\mathbf{h}$  with angle  $2k_F x_i$ , and  $\mathbf{I} \equiv \mathbf{I}_1 \perp \mathbf{h}$  is the spin at the wire end (see the Supplemental Material [40]). We find the excitations of the corresponding quantum system (magnons) by the Holstein-Primakoff representation of the effective spins by bosons [41]. Magnons, labeled by momentum  $k$ , have energies

$$\hbar\omega_k = \frac{\tilde{I}}{\sqrt{2}} \sqrt{(2J_{2k_F}^{\parallel} - J_{2k_F+k}^{\parallel} - J_{2k_F-k}^{\parallel})(J_{2k_F}^{\parallel} - J_k^{\perp})}, \quad (6)$$

where we introduced the upper index on the tensor  $J$  for its value in the helical plane ( $\parallel$ ) and in a direction perpendicular to it ( $\perp$ ). We consider first the isotropic case  $J_q^{\parallel} = J_q^{\perp}$ . The spectrum is gapless, as the two terms under the square root in Eq. (6) become zero at  $k = 0$  and  $k = 2k_F$ , respectively. Close to these values, the dispersion is linear in  $k$ , as the function  $J$  has a maximum at  $2k_F$ . The helical order critical temperature follows as (for details, see the Supplemental Material [40])

$$k_B T_c \sim I^2 J_{2k_F} = -\langle H^{\text{RKKY}} \rangle / N \equiv E_h, \quad (7)$$

so that it is given by the RKKY energy scale with the expectation value taken in the helical ground state. The critical length turns out to be extremely long and of no concern [40].

*Realizations.*—Next, we discuss three realizations of our system: magnetically doped semiconductor nanowire, such as GaMnAs; clean III-V semiconductor nanowire with high nuclear spin isotopes, such as InAs; and a chain of magnetic atoms on a superconductor surface, such as Fe on Nb. The parameters and resulting scales are summarized in Table I. We include the effective field  $\Delta_m = \alpha\beta\rho_0\tilde{I}/2$  the electrons feel once the order is established, and  $B_c = \min\{E_h/\mu_S, \Delta_m/g_e\mu_B\}$  gives a rough estimate of the critical field  $B_c$  destroying the helical order.

For a semiconductor nanowire with a moderate doping of 2%, we obtain a critical temperature of several kelvins and stability with respect to magnetic fields of order 1 T. Such nanowires can be grown very clean, with mean free paths of order microns if undoped, and are tunable by gates. Magnetic dopants will unavoidably induce some disorder. This problem is absent in the case of an undoped wire with nuclear spins, although there, the critical temperature becomes very small, 7 mK, because of the weak

TABLE I. Chosen parameter values: material, lattice constant  $a$ , electron  $g$  factor  $g_e$ , magnetic moment  $\mu_S = \tilde{I}g_s\mu$ , exchange coupling  $\beta$ , moment doping  $\alpha$ , Fermi energy  $\mu_F$ , superconducting gap  $\Delta_s$ , and the resulting scales: critical temperature  $T_c$ , critical field  $B_c$ , effective helical field strength  $\Delta_m$ , and MF localization length  $\xi$  for different realizations: the magnetic atom chain, magnetically doped nanowire, and nanowire with nuclear spins. The effective mass for GaMnAs (InAs) is  $m = 0.067m_e$  ( $0.027m_e$ ).

	Chain	Magnetic wire	Nuclear wire
Material	Fe	GaMnAs	InAs
$a$	0.3 nm	0.565 nm	0.605 nm
$g_e$	2	-0.44	-8
$\tilde{I}g_s\mu$	$2 \times 2\mu_B$	$5/2 \times 2\mu_B$	$9/2 \times 1.2\mu_N$
$\beta$	$1.6 \text{ meV nm}^3$	$9 \text{ meV nm}^3$	$4.7 \mu\text{eV nm}^3$
$\alpha$	1	0.02	1
$\mu_F$	10 meV	20 meV	1 meV
$\Delta_s$	1 meV	0.5 meV	0.1 meV
$T_c$	14 K	2 K	7.4 mK
$B_c$	5 T	0.7 T	0.4 T
$\Delta_m$	6 meV	5 meV	0.2 meV
$\xi$	4 nm	$0.4 \mu\text{m}$	$0.5 \mu\text{m}$

hyperfine interaction. We still include this realization for comparison, as establishing helical order in a nuclear wire was considered for electrons in a Luttinger liquid regime [33,34]. Like there, we expect interactions (neglected here) to enhance  $T_c$  by a factor of 2 to 4. We took InAs as the nuclear wire material and, to simplify notation in Table I, we neglected the contribution of As nuclei; thus,  $\alpha = 1$ .

An exciting possibility is offered by magnetic monoatomic chains, which can be fabricated on metal [26] or superconducting surfaces using either growth or atomic manipulation techniques with the STM [28,42]. For the latter system, the formulas we give are valid upon putting  $N_{\perp} = 1$ ,  $\alpha = 1$ , and  $A = a^2$ , with  $a$  being the interatomic distance. As an estimate, we take  $\beta/a^3 = 6 \text{ meV}$  and a hopping matrix element  $t = 10 \text{ meV}$  [26,28,42]. The stability of the helical order is rather high, comparable to the stability of the underlying superconductor, so that possible differences in these parameters are not relevant for us. What is important here is that the atomistic exchange and possible spin-orbit-based Dzyaloshinskii-Moriya interaction should be negligible for the RKKY-induced magnetism. Under these conditions, the magnetic helix pinned to the Fermi level is to be expected.

*Majorana fermions without tuning.*—From now on, we consider a helical order of localized magnetic moments to be established. These moments  $\tilde{\mathbf{I}}_i$  are aligned along the polarization vector  $\mathbf{n}(x) = \cos(2k_F x)\hat{x} + \sin(2k_F x)\hat{y}$  that is perpendicular to the helix axis  $\mathbf{h} \equiv \hat{z}$ . Such an ordered state acts back on the electrons via  $\mathcal{H}_{\text{int}}(x)$  [see Eq. (2)] that takes the form of an effective Zeeman term

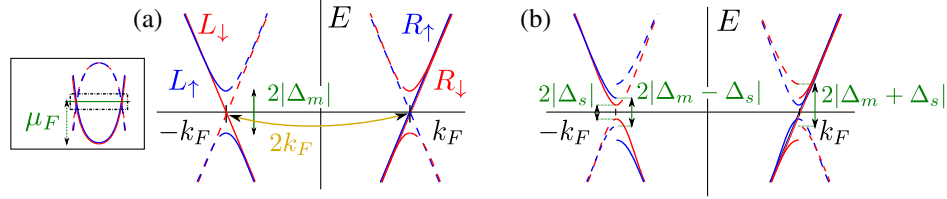


FIG. 3 (color online). (a) Electron (solid lines) and hole (dashed lines) energy spectrum around the Fermi points  $\pm k_F$  of a wire in the presence of a helical magnetic field described by  $\mathcal{H}_0 + \mathcal{H}_m$ . The inset shows the entire spectrum of  $\mathcal{H}_0$  with  $\mu_F$  being counted from the band bottom. The interaction term  $\mathcal{H}_m$  leads to a resonant scattering between right movers with spin-down  $R_\downarrow$  and left movers with spin-up  $L_\uparrow$  and results in a partial gap  $2\Delta_m$  in the spectrum [22–24,33]. Away from the Fermi points, spin-up (blue lines) and spin-down (red lines) states stay degenerate. (b) The superconducting pairing term of strength  $\Delta_s$ , which couples electron-hole states with opposite spins and momenta, gaps all branches of the spectrum [see Eqs. (10) and (11)] except for the special case  $\Delta_s = \Delta_m$ , which marks the transition between trivial and topological phases.

$$\mathcal{H}_m = \Delta_m \mathbf{n}(x) \cdot \boldsymbol{\sigma}, \quad (8)$$

where  $\Delta_m = \alpha\beta\rho_0\tilde{l}/2$  is the strength of the helical field assumed to be positive from now on.

The energy spectrum of a system described by  $\mathcal{H} + \mathcal{H}_m$  can be easily found by rewriting all electron operators in terms of slow-varying right ( $R_\sigma$ ) and left ( $L_\sigma$ ) movers:  $\psi_\sigma(x) = R_\sigma(x)e^{ik_F x} + L_\sigma(x)e^{-ik_F x}$  [43]. The helical field with a pitch  $\pi/k_F$  results in a resonant scattering between  $R_\downarrow$  and  $L_\uparrow$  [22–24,33]; see Fig. 3(a) [44]. Taking this resonance into account, we arrive at the effective Hamiltonian  $\tilde{H} = \frac{1}{2} \int dx \phi^\dagger(x) \tilde{\mathcal{H}} \phi(x)$  with the Hamiltonian density

$$\tilde{\mathcal{H}} = -i\hbar v_F \tau_3 \partial_x + \frac{\Delta_m}{2} \eta_3 (\sigma_1 \tau_1 + \sigma_2 \tau_2) + \Delta_s \eta_2 \sigma_2 \tau_1, \quad (9)$$

where the Pauli matrix  $\tau_i$  ( $\eta_i$ ) acts in left-right mover (electron-hole) space, and  $\phi = (R_\uparrow, L_\uparrow, R_\downarrow, L_\downarrow, R_\uparrow^\dagger, L_\uparrow^\dagger, R_\downarrow^\dagger, L_\downarrow^\dagger)$ . The Fermi velocity is given by  $\hbar v_F = (\partial \epsilon_k / \partial k)|_{k=k_F}$ . The diagonalization of  $\tilde{\mathcal{H}}$  gives us the bulk spectrum

$$E_\pm^{(1)} = \pm \sqrt{(\hbar v_F k)^2 + \Delta_s^2}, \quad (10)$$

$$E_\pm^{(2,\pm)} = \pm \sqrt{(\hbar v_F k)^2 + (\Delta_m \pm \Delta_s)^2}. \quad (11)$$

Here,  $E_\pm^{(1)}$  is twofold degenerate, and  $k$  is the momentum eigenvalue defined close to the Fermi points  $\pm k_F$ . The Hamiltonian  $\mathcal{H}$  belongs to the topological class BDI [45], so the system can potentially host MFs. The transition between a topological phase (with MFs) and a trivial phase (no MFs) is related to the closing and reopening of an energy gap. In our case, the system is gapless if  $\Delta_m = \Delta_s$ ; see Eq. (11) for  $E_\pm^{(2,-)}$ . Straightforward calculations [23,43] lead us to the topological criterion  $\Delta_m > \Delta_s$ . If it is satisfied, the system is in the topological phase. We note that for all three realizations considered above  $\Delta_m \gg \Delta_s$  (see Table I), thus,

the system is automatically deeply in the topological phase without any need for parameter tuning.

The MF localization length  $\xi$  is determined by the smallest gap in the system  $\xi = \hbar v_F / \Delta_s$ . If the distance  $L$  between MFs localized at opposite ends of the wire is smaller than  $\xi$ , these two MFs combine into an ordinary fermion of nonzero energy [46]. The numerical values for  $\xi$  listed in Table I are well below a micrometer. In addition, the coupling between MFs can take place via the bulk superconductor [47]. However, this channel is also efficiently suppressed in long wires.

We have tested our model numerically. As expected, the presence of MFs in the topological phase is stable against fluctuations of hopping parameters, the superconductivity strength, and the local chemical potential. We believe that disorder effects, which challenge an observation and identification of MFs [46,48–53], can be efficiently suppressed in our setup. Unlike Rashba nanowires, where the charge density is limited by the (usually weak) Rashba SOI, we can work at much higher densities, benefiting from charge impurities being screened. However, if  $\mu_F$  is increased, the critical temperature  $T_c$  goes slowly down [as  $1/k_F$ ; see Eq. (7)]. For an atom chain, which can be charged by gates, this is irrelevant, as  $T_c$  is very high to begin with. For a semiconducting nanowire, the decrease of  $T_c$  can be prevented by increasing magnetic doping.

*Conclusions.*—We have introduced a new class of superconducting systems based on RKKY interactions which feature magnetic helices with a pitch given by half of the Fermi wavelength in the quasi-one-dimensional limit. As a result, the superconductor becomes topological and hosts MFs without the need to tune the chemical potential. We have proposed candidate systems such as chains of magnetic atoms and semiconducting nanowires with nuclear spins or magnetic dopants.

We acknowledge support by the SNF, NCCR QSIT, APVV Contract No. COQI-APVV-0646-10, the U.S. National Science Foundation Grant No. NSF-DMR1104612, and the U.S. ARO.

- [1] E. Majorana, *Nuovo Cimento* **14**, 171 (1937).
- [2] A. Y. Kitaev, *Sov. Phys. Usp.* **44**, 131 (2001).
- [3] J. Alicea, *Rep. Prog. Phys.* **75**, 076501 (2012).
- [4] S. Sasaki, M. Kriener, K. Segawa, K. Yada, Y. Tanaka, M. Sato, and Y. Ando, *Phys. Rev. Lett.* **107**, 217001 (2011).
- [5] V. Mourik, K. Zuo, S. M. Frolov, S. R. Plissard, E. P. A. M. Bakkers, and L. P. Kouwenhoven, *Science* **336**, 1003 (2012).
- [6] M. T. Deng, C. L. Yu, G. Y. Huang, M. Larsson, P. Caro, and H. Q. Xu, *Nano Lett.* **12**, 6414 (2012).
- [7] A. Das, Y. Ronen, Y. Most, Y. Oreg, M. Heiblum, and H. Shtrikman, *Nat. Phys.* **8**, 887 (2012).
- [8] L. P. Rokhinson, X. Liu, and J. K. Furdyna, *Nat. Phys.* **8**, 795 (2012).
- [9] J. R. Williams, A. J. Bestwick, P. Gallagher, S. S. Hong, Y. Cui, A. S. Bleich, J. G. Analytis, I. R. Fisher, and D. Goldhaber-Gordon, *Phys. Rev. Lett.* **109**, 056803 (2012).
- [10] H. O. H. Churchill, V. Fatemi, K. Grove-Rasmussen, M. T. Deng, P. Caroff, H. Q. Xu, and C. M. Marcus, *Phys. Rev. B* **87**, 241401(R) (2013).
- [11] M. Sato and S. Fujimoto, *Phys. Rev. B* **79**, 094504 (2009).
- [12] R. M. Lutchyn, J. D. Sau, and S. Das Sarma, *Phys. Rev. Lett.* **105**, 077001 (2010); Y. Oreg, G. Refael, and F. von Oppen, *Phys. Rev. Lett.* **105**, 177002 (2010).
- [13] M. Z. Hasan and C. L. Kane, *Rev. Mod. Phys.* **82**, 3045 (2010).
- [14] X. Qi and S. Zhang, *Rev. Mod. Phys.* **83**, 1057 (2011).
- [15] P. Streda and P. Seba, *Phys. Rev. Lett.* **90**, 256601 (2003).
- [16] C. L. Kane and E. J. Mele, *Phys. Rev. Lett.* **95**, 226801 (2005).
- [17] K. Sato, D. Loss, and Y. Tserkovnyak, *Phys. Rev. Lett.* **105**, 226401 (2010).
- [18] J. Klinovaja, M. J. Schmidt, B. Braunecker, and D. Loss, *Phys. Rev. Lett.* **106**, 156809 (2011); J. Klinovaja, S. Gangadharaiah, and D. Loss, *Phys. Rev. Lett.* **108**, 196804 (2012).
- [19] J. Klinovaja, G. J. Ferreira, and D. Loss, *Phys. Rev. B* **86**, 235416 (2012).
- [20] J. Klinovaja and D. Loss, *Phys. Rev. X* **3**, 011008 (2013).
- [21] J. Klinovaja and D. Loss, *Phys. Rev. B* **88**, 075404 (2013).
- [22] B. Braunecker, G. I. Japaridze, J. Klinovaja, and D. Loss, *Phys. Rev. B* **82**, 045127 (2010).
- [23] J. Klinovaja, P. Stano, and D. Loss, *Phys. Rev. Lett.* **109**, 236801 (2012).
- [24] M. Kjaergaard, K. Wolms, and K. Flensberg, *Phys. Rev. B* **85**, 020503(R) (2012).
- [25] B. Karmakar, D. Venturelli, L. Chirolli, F. Taddei, V. Giovannetti, R. Fazio, S. Roddaro, G. Biasiol, L. Sorba, V. Pellegrini, and F. Beltram, *Phys. Rev. Lett.* **107**, 236804 (2011).
- [26] M. Menzel, Y. Mokrousov, R. Wieser, J. E. Bickel, E. Vedmedenko, S. Blügel, S. Heinze, K. von Bergmann, A. Kubetzka, and R. Wiesendanger, *Phys. Rev. Lett.* **108**, 197204 (2012).
- [27] T.-P. Choy, J. M. Edge, A. R. Akhmerov, and C. W. J. Beenakker, *Phys. Rev. B* **84**, 195442 (2011).
- [28] S. Nadj-Perge, I. K. Drozdov, B. A. Bernevig, and A. Yazdani, *Phys. Rev. B* **88**, 020407(R) (2013).
- [29] S. Nakosai, Y. Tanaka, and N. Nagaosa, *arXiv:1306.3686*.
- [30] M. A. Ruderman and C. Kittel, *Phys. Rev.* **96**, 99 (1954).
- [31] T. Kasuya, *Prog. Theor. Phys.* **16**, 45 (1956).
- [32] K. Yosida, *Phys. Rev.* **106**, 893 (1957).
- [33] B. Braunecker, P. Simon, and D. Loss, *Phys. Rev. B* **80**, 165119 (2009).
- [34] C. P. Scheller, T.-M. Liu, G. Barak, A. Yacoby, L. N. Pfeiffer, K. W. West, and D. M. Zumbuhl, *arXiv:1306.1940*.
- [35] T. Meng and D. Loss, *Phys. Rev. B* **87**, 235427 (2013).
- [36] Subbands can arise from direct hopping inside the wire or indirect hopping via the superconductor, or even from coupled Shiba states induced by the magnetic moments [28,29,37].
- [37] A. Yazdani, B. A. Jones, C. P. Lutz, M. F. Crommie, and D. M. Eigler, *Science* **275**, 1767 (1997).
- [38] A. A. Abrikosov, *Fundamentals of the Theory of Metals* (North-Holland, Amsterdam, 1988).
- [39] P. W. Anderson and H. Suhl, *Phys. Rev.* **116**, 898 (1959).
- [40] See Supplemental Material at <http://link.aps.org/supplemental/10.1103/PhysRevLett.111.186805> for details.
- [41] T. Holstein and H. Primakoff, *Phys. Rev.* **58**, 1098 (1940).
- [42] A. Yazdani *et al.* (unpublished).
- [43] J. Klinovaja and D. Loss, *Phys. Rev. B* **86**, 085408 (2012).
- [44] This is valid for a helix and breaks down close to half-filling where scattering between  $R_1$  and  $L_1$  also occurs.
- [45] S. Ryu, A. P. Schnyder, A. Furusaki, and A. W. W. Ludwig, *New J. Phys.* **12**, 065010 (2010).
- [46] D. Rainis, L. Trifunovic, J. Klinovaja, and D. Loss, *Phys. Rev. B* **87**, 024515 (2013).
- [47] A. A. Zyuzin, D. Rainis, J. Klinovaja, and D. Loss, *Phys. Rev. Lett.* **111**, 056802 (2013).
- [48] E. Prada, P. San-Jose, and R. Aguado, *Phys. Rev. B* **86**, 180503(R) (2012).
- [49] F. Pientka, G. Kells, A. Romito, P. W. Brouwer, and F. von Oppen, *Phys. Rev. Lett.* **109**, 227006 (2012).
- [50] J. Liu, A. C. Potter, K. T. Law, and P. A. Lee, *Phys. Rev. Lett.* **109**, 267002 (2012).
- [51] D. Bagrets and A. Altland, *Phys. Rev. Lett.* **109**, 227005 (2012).
- [52] D. I. Pikulin, J. P. Dahlhaus, M. Wimmer, H. Schomerus, and C. W. J. Beenakker, *New J. Phys.* **14**, 125011 (2012).
- [53] J. D. Sau and S. D. Sarma, *Phys. Rev. B* **88**, 064506 (2013).